Stromal cells in inflammatory bowel disease : perspectives of local mesenchymal stromal cell therapy

Barnhoorn, M.C.

Author: Barnhoorn, M.C.
Title: Stromal cells in inflammatory bowel disease : perspectives of local mesenchymal stromal cell therapy
Issue Date: 2020-05-07

7

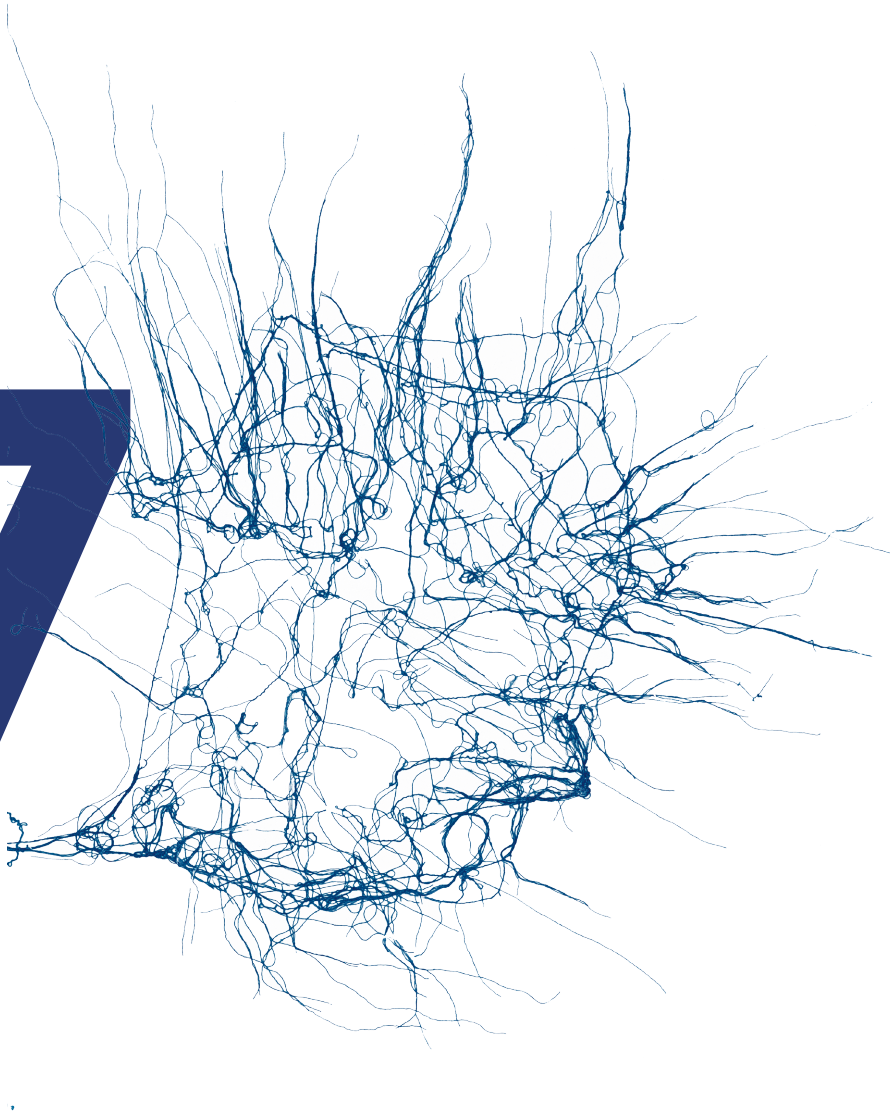

ENDOSCOPIC ADMINISTRATION OF MESENCHYMAL STROMAL CELLS REDUCES INFLAMMATION IN EXPERIMENTAL COLITIS

Marieke C. Barnhoorn
Eveline S.M. de Jonge-Muller*
Ilse Molendijk*
Mandy van Gulijk
Oscar Lebbink
Stef G.T. Janson
Mark J.A. Schoonderwoerd
Danny van der Helm
Andrea E. van der Meulen-de Jong
Lukas J.A.C. Hawinkels*
Hein W. Verspaget*

** These authors contributed equally to this work*

Inflammatory Bowel Disease 2018, 24(8); 1755-67.

ABSTRACT

Background

Mesenchymal stromal cells (MSCs) are a potential therapeutic modality in inflammatory bowel disease (IBD) because of their immunomodulatory and regenerative properties. However, when injected systemically only a small portion of the cells, if any, reaches the inflamed colon. In this study we assessed whether endoscopic injections of MSCs into the intestinal wall of the inflamed colon affect the course of experimental colitis. Furthermore, we investigated if injection of aggregated MSCs in spheroids could enhance their therapeutic ability.

Methods

Expression levels of *in vivo* MSC-aggregates and *in vitro* MSC-spheroids were compared with monolayer cultured MSCs for both anti-inflammatory and pro-regenerative factors. Subsequently, MSCs and MSC-spheroids were injected endoscopically in mice with established dextran sulfate sodium (DSS)-induced colitis.

Results

Endoscopically injected MSCs and MSC-spheroids both alleviated DSS-induced colitis. Furthermore, both *in vivo* and *in vitro* MSC-spheroids showed increased expression of factors important for immunomodulation and tissue repair, compared to monolayer cultured MSCs. Despite differential expression of these factors, MSC-spheroids showed similar clinical efficacy *in vivo* as single cell suspension MSCs. Analysis of serum samples and colon homogenates showed that local MSC-therapy resulted in increased levels of interferon-γ, indoleamine 2,3-dixoygenase and interleukin 10.

Conclusions

Endoscopic injections of MSCs and MSC-spheroids in the inflamed colon attenuate DSS-induced colitis. Our data show that endoscopic injection can be a feasible and effective novel application route for MSC-therapy in patients with luminal IBD.

INTRODUCTION

Inflammatory bowel disease (IBD) affects approximately 4 million people in Europe and the United States of America[1, 2]. IBD can be subdivided into Crohn's disease and ulcerative colitis[3, 4]. Patients with IBD suffer from abdominal pain, diarrhea and fatigue. The exact etiology of IBD is unknown but defects in immune mechanisms play an important role. Patients with Crohn's disease have an imbalance between T-helper (Th) 17 and regulatory T (Treg) cells, whereas ulcerative colitis is associated with an atypical Th2 response[3, 4]. Current therapies consist of medical treatment with immunomodulators and biologicals, and surgery to remove the severe inflamed or stenotic parts of the intestines. Despite the introduction of biological therapy there is still need for surgical intervention in 7.6-24.2% of IBD patients 5 years after diagnosis[5]. Active disease negatively affects the quality of life of IBD patients[6, 7], and therefore novel therapies are needed. One of these novel treatment options could be treatment with mesenchymal stromal cells (MSCs).

MSCs are pluripotent (stem)cells that are currently tested as a cellular therapy in several autoimmune diseases. Recent reports from clinical trials of our group and others[8, 9] showed that MSCs have promising therapeutic effects in the local treatment of refractory Crohn's disease-associated perianal fistulas. Although clinical benefit of MSC-therapy has been shown in these patients, the exact working mechanism of MSC-therapy has not been elucidated yet. Currently, it is thought that the therapeutic potential of MSCs in IBD is associated with their multilineage differentiation, regenerative capacities and especially their immunomodulatory effects. MSCs are able to act anti-inflammatory by suppressing the proliferation and activation of Th cells[10] and stimulation of Treg cells[11, 12]. Furthermore, MSCs have been reported to suppress the proliferation of B cells[13] and promote the conversion of monocytes and pro-inflammatory macrophages into anti-inflammatory macrophages[14]. Taken together these studies indicate that MSCs have immunoregulatory capacities, positioning them as an attractive potential therapy for IBD.

Although therapeutic efficacy of MSCs in the treatment of perianal fistulas has been shown, no clear therapeutic effect of systemic MSC-therapy has been established yet in luminal IBD, despite promising studies in animal models. This could be due to the fact that only a small percentage of injected MSCs engraft in proximity to the inflamed bowel after systemic infusion[15, 16]. Therefore the goal of our study was to investigate if the efficacy of MSC-therapy could be improved by local administration, using endoscopic injections of MSCs in the bowel wall and thereby directly delivering the cells to the site of inflammation. In a clinical setting, this strategy would make it possible to treat only the affected bowel segments by endoscopic MSC injection. Secondly, we wanted to investigate if we could improve the therapeutic properties of MSCs by aggregation of the MSCs in spheroids.

In the present study we show indeed a favorable expression profile in MSCs after *in vivo* and *in vitro* aggregation, and a clinical benefit of local MSC-therapy for the treatment of experimental colitis.

MATERIAL AND METHODS

MSC isolation, culture and transfection

Green fluorescent protein (GFP) expressing bone marrow MSCs were isolated from 8-12 week-old C57BL/6-Tg(CAG-EGFP)C14-Y01-FM131Osb (kindly provided by the Department of Anatomy, LUMC) and Tg(UBC-GFP)30Scha mice (The Jackson Laboratory, Bar Harbor, USA), which both express GFP in all cells, as described before[17]. In brief, mice were sacrificed and femurs were removed. The bone marrow was flushed and filtered to remove debris. After centrifugation, bone marrow derived cells were cultured in α-MEM medium (Lonza, Verviers, Belgium) supplemented with 10% fetal calf serum (FCS) (Gibco, Gaithersburg, USA), penicillin/ streptomycin (Lonza, Verviers, Belgium) and 3 mM L-glutamine (Gibco). Non-adherent cells were removed after 24 hours and the medium was refreshed every 3-4 days. For tracing experiments, part of the MSCs were transfected with a lentivirus encoding a codon optimised luciferase construct (pGL4.51, Promega Corporation, The Netherlands), kindly provided by Dr. M. Paauwe. The MSCs in the experiments were used between passage 4-9.

To confirm that the isolated cells are MSCs, they were stained with anti-CD44-APC, anti-CD29-PECy7, anti-SCA1-APC, anti-CD45-PE, anti-Ter119-V450, anti-CD105-PE and anti-CD106-PE (all BD Biosciences, San Diego, USA) and fluorescent signal was measured using the LSR II flow cytometer with Diva Software (BD Biosciences) and analysed with FlowJo software (Tree Star Inc., Ashland, USA). To test the multipotency of the isolated MSCs, cells were subjected to *in vitro* osteogenic and adipogenic differentiation assays as described previously[17]. In brief, to induce osteoblast differentiation, MSCs were cultured with 10 mM β-glycerolphosphate, 50 µg/ml ascorbic acid and 10 nM dexamethasone for 3 weeks (all Sigma-Aldrich, Zwijndrecht, The Netherlands). Adipogenic differentiation was induced by culturing MSCs in 0.5 mM 3-isobutyl-1-methylxantine, 100 µM indomethacin, 5 µM insulin and 1 mM dexamethasone for 21 days (all from Sigma-Aldrich). To confirm differentiation into adipocytes, cells were stained with Oil-Red-O (Sigma-Aldrich). To confirm osteogenic differentiation, cells were stained with Alizarin Red for calcium deposition and with Fast Blue for alkaline phosphatase activity (both Sigma-Aldrich).

MSC spheroids were generated by culturing MSCs in 96-well U bottom cell culture plates (Greiner Bio-One BV, Alphen a/d Rijn, The Netherlands) for 24 or 48 hours (1,000 cells/

well) in full medium containing 0.24% methylcellulose (Sigma-Aldrich). In indicated *in vitro* experiments MSCs were stimulated with 500 U/mL recombinant mouse TNF-α (R&D systems, Minneapolis, USA) and/or 40 U/mL recombinant mouse IFN-γ (Biolegend, San Diego, USA) for 24 hours.

Intraperitoneal aggregation and endoscopic treatment of colitis with MSCs

To investigate *in vivo* aggregate formation, $2x10^6$ MSCs were injected intraperitoneally in C57BL/6Jico mice (Charles River Laboratories, Saint-Germain-Nuelles, France). To trace MSCs *in vivo* 100 mg/kg luciferin (Bachem, Bubendorf, Switzerland) was injected intraperitoneally, and mice were imaged on the IVIS Lumina-II (Caliper Life Sciences, Hopkinton, USA). After 5 days mice were sacrificed and MSC-aggregates were collected in PAXgene RNA solution (Qiagen, Hilden, Germany) for RNA isolation or in 4% formalin for immunohistochemical analysis.

To induce colitis, female C57BL/6Jico mice were given 2.5% dextran sulphate sodium (DSS; MW 36000-50000kDA; MP Biomedicals, Brussel, België) in the drinking water for 7 days. DSS was refreshed every other day. Body weight was measured daily, and at day 5, mice were treated with $2x10^6$ MSCs or 2,000 MSCs in spheroids (equivalent to $2x10^6$ cells) in 200 µl PBS (n=18-19 mice/group). In the control group, mice received 200 µl PBS. MSCs were injected in 4 spots (50 µl/spot), one in every quadrant of the distal bowel wall with a 30 G needle during endoscopy using a high-resolution miniaturized colonoscope system (Karl Storz, Tuttlingen, Germany). Mice were sacrificed 4 (n=10-11/group) or 6 days after treatment (n=8/group), then colons were opened longitudinally and the macroscopic disease score[17, 18] was established for each mouse. This score was composed of the presence of loose stool (0-3), visible faecal blood (0-3) and macroscopic inflammation (0-3), resulting in a maximum score of 9. Bioluminescent imaging was performed in 4 mice to show the localisation of injected MSCs.

Flow cytometry

Lamina propria colonic cells were obtained by incubation of colonic tissue in 5 mM EDTA (Merck, Darmstadt, Germany) and 1 mM dithiothreitol (Sigma-Aldrich) for 20 minutes, followed by matrix digestion in Liberase TL solution (Roche, Indianapolis, USA) for 30 minutes at 37 °C. Single cell suspensions were measured on LSR II flow cytometer as described above.

RNA isolation and quantitative PCR

RNA was isolated from cells or tissue using NucleoSpin RNA Kit (Macherey Nagel, Düren, Germany) according to the manufacturers' protocol. RNA concentration and

purity were determined using NanoDrop 3300 (ThermoFisher Scientific, Waltham, USA). cDNA was generated using RevertAid First Strand cDNA Synthesis Kit (ThermoFisher Scientific) according to manufacturers' instructions. Quantitative PCR (qPCR) reactions were carried out using SYBR Green (Biorad, Hercules, USA) and primers for GFP, CD45, stromal cell-derived factor (SDF)-1, C-X-C chemokine receptor type 4 (CXCR-4), C-C motif ligand chemokine ligand (CCL)2, CD200, vascular endothelial growth factor (VEGF)-A, VEGF receptor (VEGFR)-1, hepatic growth factor (HGF), interferon (IFN)-γ, indolamine 2,3-dioxygenase (IDO), interleukin 18-binding protein (IL-18bp), intracellular adhesion molecule (ICAM)-1, epidermal growth factor (EGF), transforming growth factor (TGF)-β1, TGF-β2, TGF-β3, cytokeratin-20 (CK20), leucine-rich repeat-containing G-protein coupled receptor 5 (LGR5) (all Invitrogen custom primers, Carlsbad, USA) and glyceraldehyde 3-phosphate dehydrogenase (GAPDH) (Qiagen) (Supplementary digital content 1, primer sequences). cDNA samples were subjected to 40 cycles real-time PCR analysis as previously described[19]. All values were normalized for cDNA content by GAPDH expression.

Cytokine measurement

Colonic tissue was homogenised in RIPA buffer (150 mM NaCL, 1% NP-40, 0.25% deoxycholate, 0.1% SDS, 50 mM Tris (pH 8.0), 2 mM EDTA, 1 mM NaVO4, 10 mM NaF and 1 mM sodium orthovandate (BDH Laboratory, Poole Dorstet, UK)) using TissueLyser LT (Qiagen). Total protein content was determined using a BCA protein assay kit (ThermoFisher Scientific). Total levels of VEGF and TGF-β1 were determined by using commercially available ELISA Duosets (R&D systems) as described before[20]. Briefly, wells were incubated overnight with capture antibody. After blocking, samples were incubated for 2 hours, followed by biotinylated antibodies and color development (Color reagent pack, R&D systems). Absorption was measured at 450nm. Additional cytokine levels in colon homogenates and blood were obtained using U-PLEX assay (Mesoscale, Rockville, USA). All cytokine levels in colon homogenates were corrected for total protein amount. Serum amyloid A (SAA) levels were measured using a commercial ELISA kit according to the manufacturer's instructions (Tridelta Development Ltd, Ireland).

Western blot analysis

Western blot analysis were performed as described before[19]. Briefly, equal amounts of proteins were separated on 10% SDS-polyacrylamide gel electrophoresis under reducing conditions. Subsequently, separated proteins were transferred to polyvinylidine fluoride membranes (Whattman, Dassel, Germany). Non-specific binding was blocked in 5% milk in tris-buffered saline with 0.05% Tween-20 (TBST). Blots were incubated overnight with primary antibodies: goat anti-CD200 (R&D systems), rat anti-IDO (BioLegend) or rat anti-CXCR-4 (BD Biosciences). Bands were visualized using horseradish peroxidase conjugated

secondary antibodies and enhanced chemiluminescence detection kit (Roche, Indianapolis, USA). Blots were stripped and reprobed with mouse anti-GAPDH antibody (ThermoFisher Scientific) as a loading control. Densitometric analysis was performed with Image Lab Biorad software version 5.2.

Immunohistochemical analysis

Haematoxylin and eosin staining of the colons was used to visualize the microscopic signs of inflammation in distal colon. The IBD histology score consisted of muscularis mucosae thickness (0-3), immune cell infiltrate (0-3), crypt architecture (0-3) and presence of goblet cells (0-1). Scoring was performed blinded to treatment by 2 individual observers.

Immunohistochemical stainings were performed as described before[17] using primary antibodies against GFP (goat; Rockland, Limerick, Ireland), Ki67 (rabbit; Merck), cleaved-caspase 3 (rabbit; Cell Signaling Technologies, Boston, USA), CD3 (rabbit; Dako, Santa Clara, USA), Foxp3 (rat; ThermoFisher Scientific), Ly6G (rat; Biolegend), F4/80 (rat; BD Biosciences) and MBP (rat; kindly provided by Dr. Lee, Mayo Clinic, USA). In brief, sections were deparaffinised, rehydrated and incubated in 0.3% H_20_2/methanol for 20 minutes to block endogenous peroxidase. Antigen retrieval was performed using 0.01 M sodium citrate (pH 6.0) and primary antibodies were incubated overnight. The next day, slides were incubated for 60 minutes with biotinylated secondary antibody (Dako) followed by incubation with Vectastain (Vector Laboratories, Burlingame, USA) and DAB (Dako) staining for 10 minutes. All slides were counterstained with haematoxylin. For Foxp3-staining slides were blocked with Teng-T (10mM Tris, 5mM EDTA, 0.15M NaCL, 0.25% gelatin, 0.05% Tween-20, pH 8). For MBP-staining slides were incubated with Pepsin Solution Digest-all (Invitrogen) for antigen retrieval. The amount of MBP-positive cells in the colon was evaluated by two independent researchers blinded to treatment groups using a score ranging from 0-4 for both the mucosal and submucosal layer. To evaluate Foxp3-staining, three microscopic images of the distal colon were made with 10x magnification and positive cells were counted in the mucosal and submucosal layer using ImageJ software (National Institutes of Health, USA).

Statistical analysis

Data are presented as mean ± standard error of the mean (SEM). Differences between two groups were calculated using Student's t-test or Mann-Whitney tests, whereas for more than two groups one-way ANOVA or Kruskal-Wallis tests were used followed by Dunnett's multiple comparison test. Pearson's correlation test was used to analyse the correlation coefficient. All analyses were performed in GraphPad Prism software. P-values ≤ 0.05 were considered statistically significant.

Ethical Considerations

All animal experiments were approved by the animal ethical committee of the Leiden University Medical Center (LUMC). Mice were housed in individually ventilated cages and had access to drinking water and food *ad libitum*.

RESULTS

MSC isolation and characterisation

MSCs were isolated from the bone marrow of GFP-expressing mice and expression of mesenchymal stem cell precursor markers on the cells was confirmed using flow cytometry. MSCs showed expression of GFP, CD29, CD44, SCA-1, CD105 and CD106, while the haematopoietic marker CD45 and the erythrocyte marker TER-119 were absent (Supplementary Figure 1A). Next, to confirm their multipotency, cells were subjected to differentiation assays, showing their ability to differentiate into adipocytes and osteoblasts (Supplementary Figure 1B).

Intraperitoneally injected MSCs aggregate into spheroids and show upregulation of immune regulating and tissue repair genes

To analyse how intraperitoneally injected MSCs behave, the expression profiles of the *in vivo* formed aggregates were compared to MSCs from *in vitro* monolayer cultures. Five days post-injection of MSCs in single cell suspension, abdominal MSC-aggregates could be detected, which appeared as small clusters with a white-yellowish colour (Figure 1A). Bioluminescent imaging confirmed the presence of luciferase-expressing MSCs in these spots (Supplementary Figure 2A). These aggregates could be isolated and subsequently cultured *in vitro*. Spindle shaped GFP-positive cells, were present in culture after five days (Figure 1B). In mice with DSS- and trinitrobenzene sulfonic acid solution (TNBS)-induced colitis similar MSC-aggregates were formed after intraperitoneal injection of MSCs (Supplementary Figure 2B). MSC-aggregates directly isolated from healthy mice, without culturing, were used for immunohistochemistry and qPCR. GFP immunohistochemistry and qPCR confirmed their origin (Figure 1C and Supplementary Figure 2C). Low levels of CD45 RNA could also be detected in the MSC-aggregates by qPCR (Supplementary Figure 2D). To investigate the expression pattern of *in vivo* aggregated MSCs, RNA form the isolated MSC spots was evaluated by qPCR for genes involved in immunomodulation and tissue repair and compared to the identical MSCs which were injected. Significantly higher RNA expression levels of the anti-inflammatory cytokine TGF-β1 and CD200, a transmembrane glycoprotein that stimulates the differentiation of T cells to Treg cells[21], were found in the *in vivo* aggregates compared to the *in vitro* MSCs. Also RNA expression of factors involved in tissue repair, like VEGF and HGF were upregulated in the *in vivo* MSC-

aggregates. CXCR-4 gene expression, important for the homing of MSCs towards damaged tissue[22], was also significantly upregulated in the isolated aggregates. SDF-1, a ligand for CXCR-4, CCL-2, important for the recruitment of T cells, and VEGFR-1 expression were similar between *in vitro* MSCs and *in vivo* MSC-aggregates (Figure 1D). No correlation was found between the expression of these genes and the amount of CD45 RNA in these spots, indicating that the expression is not due to the low, but detectable amount of contaminating CD45+ cells (data not shown). These results indicate that MSCs after *in vivo* aggregation show a favourable RNA expression profile (anti-inflammatory and pro-regenerative) for the treatment of colitis.

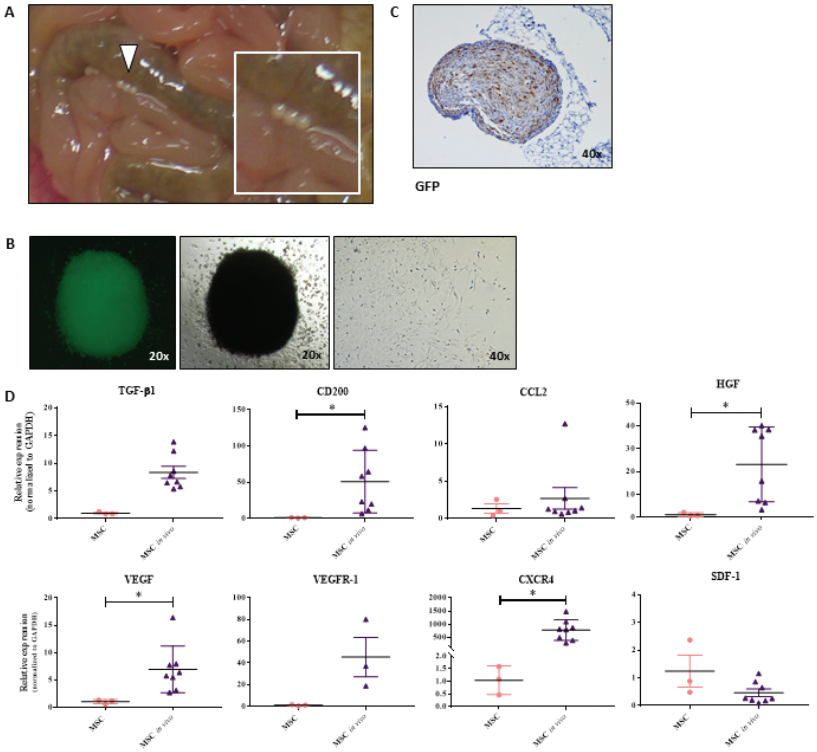

FIGURE 1. MSC-aggregates, formed after intraperitoneal injection, show upregulation of immune regulatory and tissue repair genes. (A): MSC-aggregates in the murine abdomen 5 days after injection. (B): Immunofluorescent and bright-field images of MSC-aggregates in culture confirming the presence of GFP-positive MSCs. Spindle shaped cells grow from the aggregate after 5 days of culture (right picture). (C): GFP immunohistochemistry confirming the presence of MSCs in the aggregates. (D): qPCR comparing isolated RNA from *in vitro* MSCs (n=3) with abdominal *in vivo* MSC-aggregates (n=3-8). RNA expression levels are determined in triplicate and normalized to GAPDH. Relative expression of MSCs *in vivo* is calculated compared to *in vitro* MSCs (set to 1). Data are expressed as mean ± SEM. *$p \leq 0.05$.

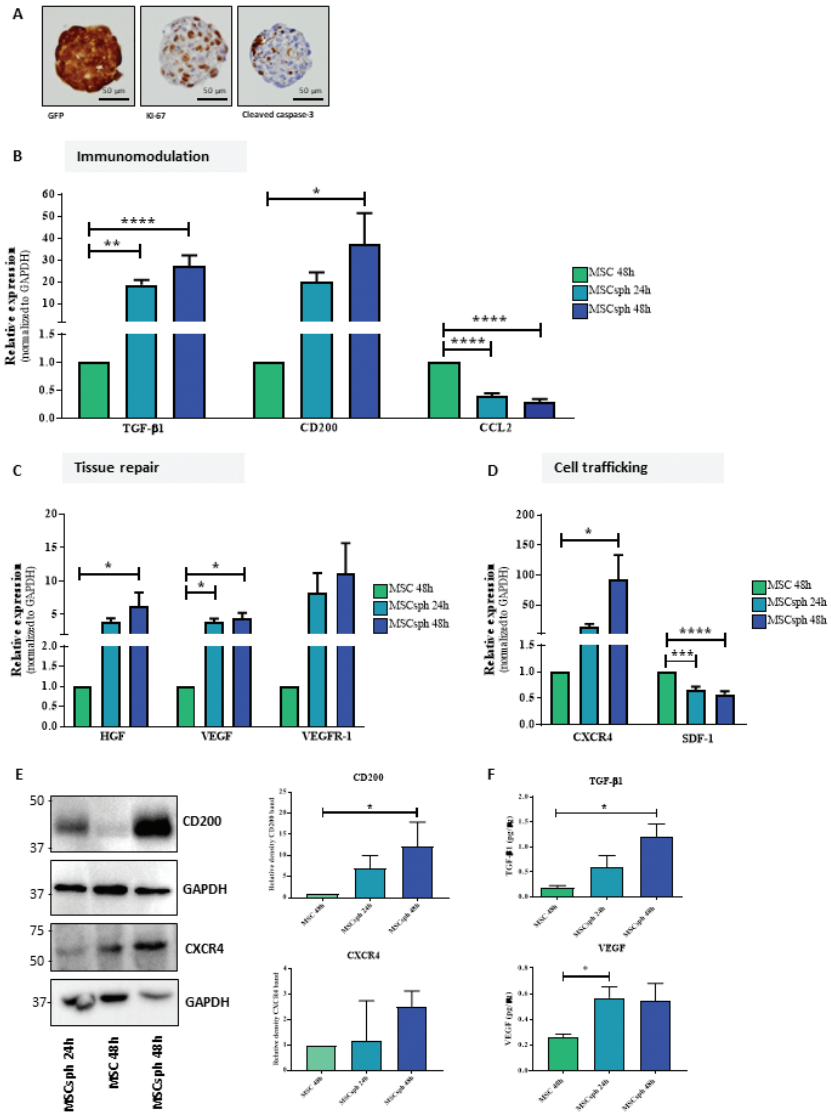

FIGURE 2. *In vitro* aggregation of MSCs in spheroids shows differential expression of genes involved in immunomodulation, tissue repair and cell trafficking. (A): Immunohistochemistry on embedded *in vitro* MSC-spheroids for GFP, KI-67 and cleaved caspase-3. (B/C/D): qPCR comparing expression levels of MSCs cultured in monolayer for 48 hours (MSC 48h), in spheroids for 24 (MSCsph 24h) and 48 hours (MSCsph 48h) for genes involved in immunomodulation (B), tissue repair (C) and cell trafficking (D). The data are the result of 6 independent experiments in triplicate. Expression levels are normalized to GAPDH and compared to MSC 48h. (E): Western blot analysis for CD200 and CXCR-4. GAPDH is used as a loading control. A representative Western blot from three independent experiments is shown. Quantifications are corrected for GAPDH. (F): TGF-β1 and VEGF levels in cell lysates of MSC 48h, MSCsph 24h and 48h measured by ELISA. Experiments are performed in triplicate. All data are expressed as mean ± SEM. * $p \leq 0.05$, ** $p \leq 0.01$, *** $p \leq 0.001$, **** $p \leq 0.0001$.

MSCs aggregated in spheroids *in vitro* mimic their *in vivo* counterparts

In order to confirm the altered expression pattern of the aggregated MSCs *in vitro*, GFP expressing MSCs were cultured in 3-dimensional spheroids (1,000 MSCs/ spheroid). After 48 hours MSCs aggregated into single spheroids in every well (Supplementary Figure 3A). These MSC-spheroids showed high expression of the proliferation marker Ki-67 and low levels of the apoptotic marker cleaved caspase-3 (Figure 2A), indicating that cells are viable and proliferating. Next, MSCs cultured in monolayer were compared with MSCs cultured in spheroids for 24 and 48 hours on RNA expression levels for 12 genes involved in immunomodulation, tissue repair and cell trafficking. Expression levels of anti-inflammatory TGF-β1 and TGF-β2 were significantly higher in the spheroids compared to MSCs cultured in monolayer, while TGF-β3 expression did not differ (Figure 2B and Supplementary Figure 3B). In addition, CD200 showed an upregulation in the MSC-spheroids, corresponding to what was observed in the *in vivo* aggregates. CCL-2 showed a downregulation in spheroids compared to monolayer cultured MSCs. In contrast, genes involved in tissue repair, like HGF, VEGF and VEGFR-1 showed an upregulation when MSCs were cultured in spheroids (Figure 2C). CXCR-4 RNA expression was also strongly increased in the spheroids, while SDF-1 was slightly downregulated (Figure 2D).

To confirm that increased RNA expression results in increased protein expression, CD200, CXCR-4, TGF-β1 and VEGF protein levels were evaluated using western blot or ELISA. These data indeed confirm their increased expression in spheroids (Figure 2E and F). Overall, these results indicate that *in vitro* aggregated MSCs in spheroids have a more favourable expression pattern, similar to *in vivo* aggregated MSCs, to alleviate colitis.

Endoscopically injected MSCs and MSC-spheroids alleviate DSS-induced colitis

The therapeutic effects of *in vitro* cultured MSCs in spheroids and in monolayer were investigated in a DSS mouse model for colitis. To increase their potential effectiveness, $2x10^6$ GFP-expressing MSCs cultured in single cell suspension or in spheroids (1,000 MSCs/spheroid) were injected during endoscopy in four spots in the inflamed distal colon at day 5 of DSS administration. Successful injections during endoscopy were confirmed by the observation of a blister in the bowel wall (Figure 3A and Supplementary digital content, which demonstrates endoscopic injection in the bowel wall). Bioluminescence imaging using luciferase-expressing MSCs was performed. Both MSCs and MSC-spheroids were detectable up to six days after endoscopic injection in the distal colon (Figure 3B), indicating successful injection and survival of the cells.

Mice treated with MSCs or MSC-spheroids showed a higher relative body weight at day 9, 10 and 11 compared to the PBS-treated group (Figure 3C). Four or six days after start

of treatment, the mice were sacrificed and the colons were evaluated. In agreement with the significantly higher body weight after MSC-therapy, the macroscopic disease score was lower in mice treated with local MSCs and MSC-spheroids (Figure 3D) at day 6. For tracing MSCs, part of the lamina propria cells of the colon were isolated for flow cytometric analysis of GFP. 16 out of 21 (76%) mice injected with MSCs or MSC-spheroids had GFP-positive cells in the lamina propria 4 days after treatment, whereas no GFP-positive cells were observed in the control mice (Figure 3E).

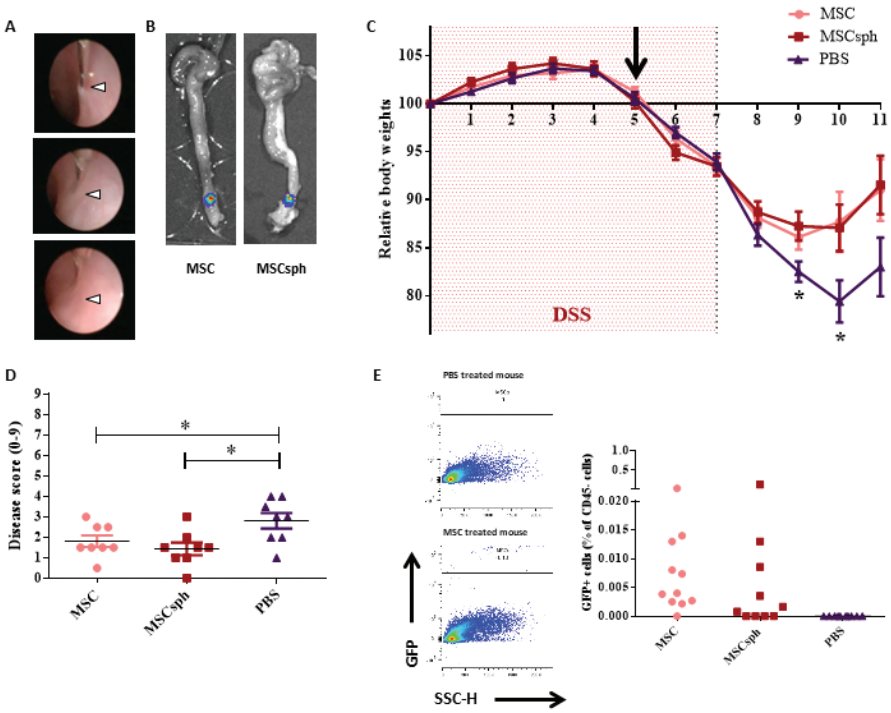

FIGURE 3. Endoscopic injections of MSCs alleviate DSS-induced colitis. (A): Sequential pictures of an endoscopic injection of MSCs in the bowel wall, showing the appearance of a submucosal blister. (B): Bioluminescent images of colons 6 days after endoscopic injections with luciferase-expressing MSCs or MSC-spheroids (MSCsph), showing the presence of MSCs in the distal colon. (C): Relative body weights of the mice during the experiment (n=18-19 mice/ group). Mice are endoscopically treated at day 5 and sacrificed at day 9 (n=10-11/ group) or at day 11 (n=8/ group). A significant higher bodyweight is observed in both MSC-treatment groups at day 9 and 10 compared to the PBS-treated group. (D): A higher macroscopic IBD disease score, based on the presence of loose stool, fecal blood and macroscopic signs of inflammation, is observed in PBS-treated mice. (E): Flow cytometry analysis of lamina propria cells isolated from the colon confirms the presence of GFP-positive MSCs in MSC-treated mice. Data are expressed as mean ± SEM. *$p \leq 0.05$.

Histological analysis revealed a lower IBD histology score in MSC-treated mice compared to the control mice (Figure 4A). To confirm the presence of MSCs in the bowel wall, section were stained for GFP. These data showed the presence and engraftment of MSCs until the end of the experiment, confirming the bioluminescent imaging and flow cytometry data. Clusters of GFP-positive cells were found both in the submucosal area and at the serosal side of the colon in mice injected with MSCs and MSC-spheroids six days after injection (Figure 4B). Circulating SAA levels, a general inflammation marker, were determined as well. Our data showed upregulation of SAA in mice with DSS-induced colitis compared to healthy mice. Lower serum SAA levels were detected in mice treated with MSC-spheroid-therapy compared to the control group (Figure 4C). Taken together, these data show that locally applied MSCs and MSC-spheroids are both able to ameliorate DSS-induced colitis, including improvement in the macro- and microscopic IBD score.

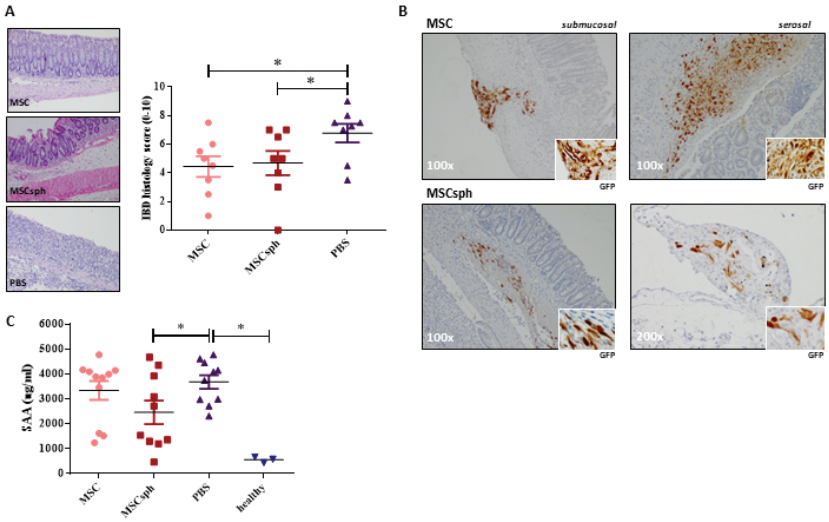

FIGURE 4. MSCs in the submucosal and serosal layer of the bowel lower microscopic signs of inflammation. (A): Lower IBD histology scores (muscularis mucosae thickness, immune cell infiltrate, crypt architecture and presence of goblet cells) are observed in mice treated with MSCs. (B): MSCs are detected in both the submucosal and serosal layer of the colon up to 6 days after endoscopic injection using GFP-staining. Magnification x100 or x200, inserts higher magnification. (C): The systemic inflammation marker SAA is strongly elevated in mice with DSS-induced colitis. Treatment with MSC-spheroids significantly lowers the SAA levels in the blood. Samples are measured in duplicates. Data are expressed as mean ± SEM. *$p \leq 0.05$.

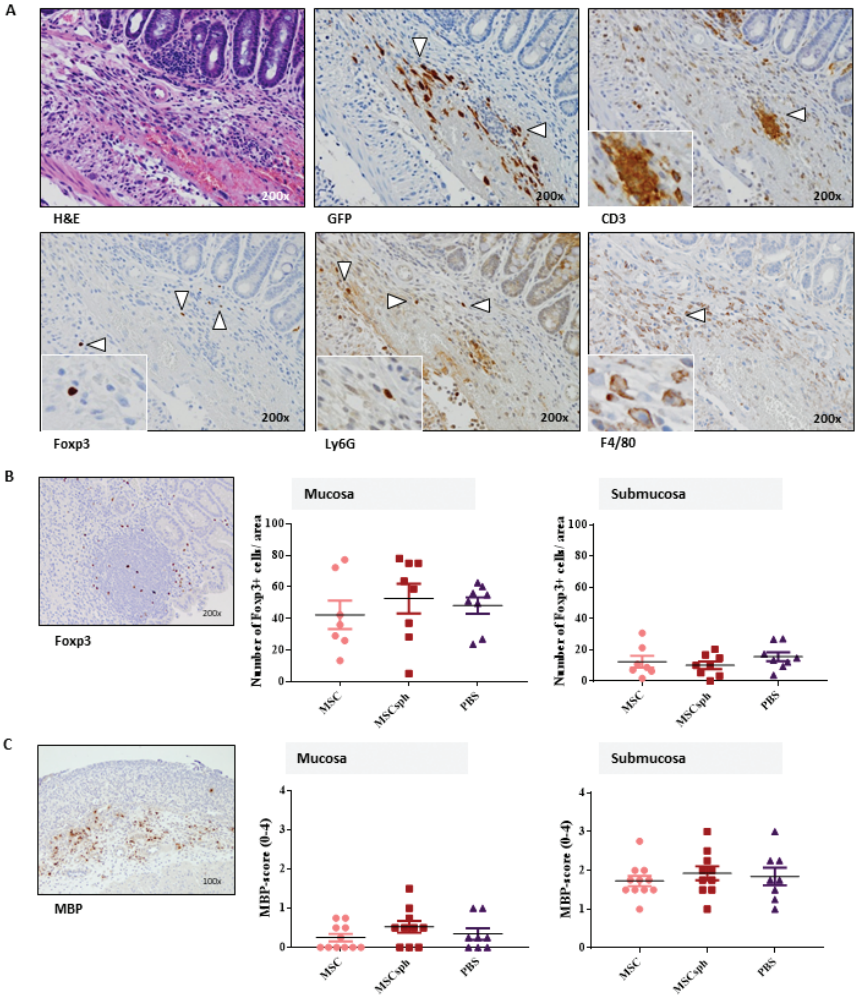

FIGURE 5. CD3- and F4/80-positive cells surround MSCs injected in the bowel wall. (A): Immunohistochemical stainings for GFP reveal the localization of MSCs after endoscopic injection. CD3-, Foxp3-, Ly6G- and F4/80-stainings show the presence of respectively T cells, Treg cells, neutrophils and macrophages in proximity of the MSCs. White arrowheads indicate positive cells. Magnification x200, inserts higher magnification. (B/C): Immunohistochemical staining with anti-Foxp3 (B) in order to detect Treg cells and anti-MBP (C) to detect eosinophils. Foxp3-positive nuclei are quantified using ImageJ. The percentage of MBP-positive cells is determined by two observers blinded to treatment. No differences in the number or percentage of positive cells in the mucosa (left panel) or submucosa (right panel) is detected between the treatment groups. Data are expressed as mean ± SEM.

T cells and macrophages surround MSCs injected into the bowel wall

Since MSCs and MSC-spheroids can modulate immune cells, colonic tissue sections were analysed for various subtypes of immune cells. CD3-, Foxp3-, Ly6G- and F4/80-stainings were performed to identify respectively T cells, Treg cells, neutrophils and macrophages near injected MSCs (Figure 5A). A substantial amount of CD3-positive cells was found in proximity of MSC-clusters. In contrast, only a few Foxp3-positive Treg cells were seen close to the MSCs. No differences were found between the number of Treg cells in the distal colon of the different treatment groups (Figure 5B). Also the number of eosinophils was not affected by MSC-therapy (Figure 5C). A few Ly6G-positive neutrophils could also be detected in close proximity to the MSCs. F4/80+ macrophages on the other hand were well detectable near the MSCs. No differences between the amount and type of immune cells surrounding MSCs injected in monolayer or as spheroids was observed. These data indicate that in DSS-induced colitis T cells and macrophages are the predominant cell types surrounding MSCs in the bowel wall. Ki67-staining showed normal crypt proliferation in the three treatment groups (Supplementary Figure 4A), while no ectopic crypt formation was detected. No differences between the RNA expression of the stem cell marker LGR5 were found between MSC- and PBS-treated colon samples. In contrast higher CK20 expression, a marker for differentiated epithelial cells, could be detected in the colon of mice treated with MSC-spheroids, suggesting more epithelial repair in these mice (Supplementary Figure 4B).

Local MSC-therapy induces IFN-γ, IDO and IL-10 upregulation

To assess the immunomodulatory effects of local MSC-therapy on DSS-induced colitis, cytokines in serum and colon homogenates were measured. The levels of the pro-inflammatory cytokines IL-17, IL-6, IL-8 and TNF-α were elevated in the colon of mice receiving DSS in the drinking water. MSC-therapy showed a consistent tendency of reduced levels of these cytokines in the colon four days after treatment (Figure 6A). No differences in VEGF or TGF-β levels where found in the colon of mice injected with MSCs or MSC-spheroids (data not shown). Six days after treatment colon homogenates showed comparable IL-17, IL-6, IL-8 and TNF-α levels between the three treatment groups (data not shown). Higher levels of the anti-inflammatory cytokine IL-10 were found in the serum of mice treated with MSCs, particular in the MSC-spheroid group (Figure 6B). Serum IFN-γ levels were below the detection limit in all PBS-treated mice, but in 7 out of 10 MSC-treated mice detectable levels were observed (Figure 6C). Moreover, in colon homogenates higher IFN-γ levels were observed in mice that received MSC-therapy (Figure 6C), although this did not reach statistical significance. IFN-γ is known to upregulate a series of anti-inflammatory IFN-γ-inducible genes in immune cells, DSS-damaged epithelial cells and in MSCs[23]. These genes include the anti-inflammatory proteins IDO and IL-18bp. Our data show indeed

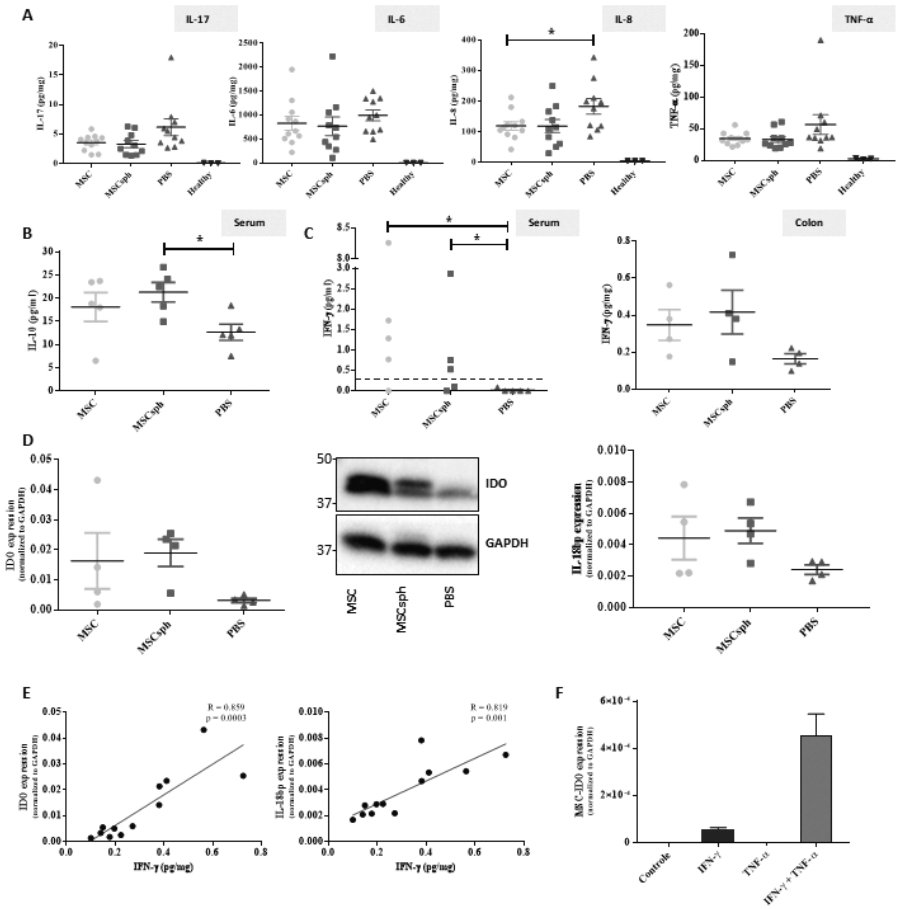

FIGURE 6. Endoscopic injections of MSCs alter cytokine and enzyme production. (A): Cytokine levels of IL-17, IL-6, IL-8 and TNF-α in the colon are upregulated after DSS-induced colitis. Local MSC-therapy significantly reduces IL-8 levels. (B): IL-10 levels in the serum are significantly higher in mice treated with MSC-spheroids compared to PBS. (C): IFN-γ is only detectable in the serum of mice treated with MSCs or MSC-spheroids (left panel). IFN-γ levels are also higher in colon homogenates after MSC-therapy (right panel). (D): RNA expression levels of IDO (left panel) and IL18bp (right panel) are elevated in MSC-treated mice 6 days after MSC-therapy. Higher RNA expression levels for IDO after MSC-therapy are confirmed on protein level by western blot (middle panel). (E): IFN-γ levels in the colon are significantly correlated with IDO and IL-18bp expression levels, R = 0.859 and 0.819 respectively, $p \leq 0.001$. (F): MSCs are stimulated *in vitro* for 24h with IFN-γ, TNF-α or a combination of both, and IDO expression is determined. IFN-γ stimulation induces IDO expression, which is further enhanced by addition of TNF-α. Data are expressed as mean ± SEM. *$p \leq 0.05$.

upregulation of RNA levels of IDO and IL-18bp in the colon of MSC-treated mice (Figure 6D). The upregulation of IDO in the colon of MSC-treated mice was confirmed by western blot analysis (Figure 6D). Interestingly, the expression levels of both IDO (R = 0.859) and IL-18bp (R = 0.819) were directly correlated with the level of IFN-γ in the colon homogenates six days after treatment (Figure 6E). The same trend was observed four days after treatment, with a higher IFN-γ level corresponding with a higher IDO expression (Supplementary Figure 5A and B). In order to investigate if the injected MSCs are indeed capable of inducing IDO production after stimulation with cytokines we performed additional *in vitro* experiments. MSCs, stimulated with IFN-γ showed a remarkable upregulation of IDO expression, which could even be further enhanced by combining IFN-γ with TNF-α stimulation (Figure 6F). Taken together, these results suggest that local MSC-therapy can induce an anti-inflammatory response possible via activation of IFN-γ, IDO and IL-10 pathways.

DISCUSSION

In this study we have shown that local, endoscopic administration of MSCs is feasible and effective in mice with experimental colitis. Furthermore, we have demonstrated that MSCs in aggregates (*in vivo* or *in vitro*) express increased levels of immunosuppressive and tissue regenerative factors, like TGF-β1, CD200, HGF and VEGF. Interestingly, our data also showed that generating *in vitro* spheroids is not required to obtain similar clinical effects.

MSC-therapy is a promising novel approach for the treatment of perianal fistulas in Crohn's disease, based on recent clinical data[8, 9]. Besides highlighting the feasibility and safety of local MSC-therapy in IBD, these trials also show a response rate up to 80% in patients with perianal fistulas refractory for standard treatment. Potentially, MSC-therapy could also be beneficial for the treatment of luminal IBD, but several improvements with regard to homing and immune regulatory properties should be made to enhance their efficacy. Our results demonstrated that aggregation of MSCs in spheroids enhances the expression of at least TGF-β1, CD200, HGF, VEGF and CXCR-4. Upregulation of CXCR-4, in addition to the upregulation of anti-inflammatory tumor necrosis factor-inducible-6 (TSG-6), stanninocalcin-1 and leukemia inhibitory factor, was also observed by others in human MSCs cultured in spheroids[24]. These spheroids were also found to be more effective in suppressing inflammation in a mouse model of zymosan-induced peritonitis, when compared to monolayer cultured MSCs[24]. Surprisingly, our results showed that in experimental colitis administration of MCSs aggregated in spheroids *in vitro*, did not result in better clinical responses than single cell MSCs. Although *in vitro* expression profiles showed an upregulation of VEGF and TGF-β1 in MSC-spheroids, similar levels of VEGF and TGF-β1 were found in the bowel wall of mice after endoscopic injection with MSCs or MSCs

aggregated in spheroids. These data together could suggest that in an acute disease model the high cytokine levels are sufficient to activate the anti-inflammatory and pro-regenerative features of MSCs and polarize MSCs in a favourable phenotype for treating autoimmune diseases[25]. However, this might imply that in chronic conditions it could still be critical to pre-activate the MSCs *in vitro* by culturing in spheroids or pre-stimulate them with pro-inflammatory cytokines. Another explanation for the comparable results between MSCs and MSC-spheroids *in vivo* is the spontaneous aggregation of MSCs that was observed after injection in the bowel wall.

Detection of MSCs after administration has been proven difficult and most studies show that only a small number of MSCs, if any, will reach the inflamed tissue[15, 17, 26]. Here we could show that MSCs injected as single cells or in spheroids are detectable until the end of the experiment, six days after injection. Moreover, we could show that the MSCs are localised in the submucosal and serosal area and co-localize with T cells and macrophages. In a previous study, MSCs injected intraperitoneally in mice with experimental colitis were also found to be surrounded by macrophages and T cells, besides to some B cells and Ly6G positive cells[26]. The close proximity of endoscopically injected MSCs to colonic immune cells gives them the opportunity to modify these cells directly through cell-to-cell contact and indirectly through the production of short-living cytokines, like TGF-β1 and CD200.

Several cytokines have been proposed to mediate the regenerative and anti-inflammatory features of MSCs. Manieri and colleagues[27] recently showed that endoscopic applied MSCs could promote intestinal repair and angiogenesis in intestinal wounds, mainly by short-living factors, like VEGF, one of the factors that was upregulated by aggregation into spheroids. Sala and colleagues[26] reported TSG-6 to be responsible for the clinical effect of intraperitoneally injected MSCs in experimental colitis. Our data indicate that not a single pathway, but the interplay between several pathways is most likely responsible for the anti-inflammatory effects of MSCs. This will probably also depend on the disease model, host and donor. Our study showed that the pathways of IFN-γ, IDO and IL-10 are all involved in the anti-inflammatory mechanisms of local MSC-therapy in acute colitis. No significant differences in the levels of IL-17, IL-6 and TNF-α in the colon between the MSC-treated mice and controls were observed, which could imply that these cytokines correlate with resolution of inflammation rather than being directly related to the MSC-therapy. However, higher levels of IFN-γ were observed in MSC-treated mice. The role of IFN-γ in experimental colitis and MSC-therapy is complex. IFN-γ is known for both its pro-inflammatory and anti-inflammatory effects, but especially at early stages of inflammation, IFN-γ has homeostatic functions by stimulating Paneth cells to release antimicrobial peptides[28] and modulating anti-inflammatory molecules like IDO and IL-18bp[23]. Important with regard to IBD is that

IFN-γ is capable of suppressing Th17 cells and thereby restoring the balance between Th17 and Th1 cells[29]. In line with our observations, in a mouse model of rheumatoid arthritis enhanced levels of IFN-γ where measured in the spleen of mice treated with combined MSC- and type I regulatory T cell (Tr1)-therapy compared to mice treated with Tr1-therapy alone[30]. IFN-γ levels strongly influence the suppressive effect of MSCs by inducing IDO production. Recently, the importance of IDO in the working mechanism of MSCs in IBD was revealed, by showing that MSCs dampen the inflammatory response of mucosal T cells in Crohn's disease through the upregulation of IDO activity[31]. MSCs are known to stimulate certain cell types, like T cells and macrophages to produce IL-10, through the production of IDO or prostaglandin E2[32]. Previously it was found that human MSCs are better capable than murine MSCs in upregulating IDO[33]. However, in the current study we showed that murine MSCs are also able to increase their IDO expression after IFN-γ stimulation and even further after the addition of other cytokines next to IFN-γ. Taken together, these data indicate that local MSC-therapy alleviates experimental colitis possibly through the elevation of IFN-γ, leading to increased IDO production by MSCs and eventually IL-10 production by immune cells.

In conclusion, our data showed the potency of local MSC-therapy for the treatment of luminal IBD. Endoscopically applied MSCs can be used as a novel application route for luminal IBD with substantial advantages compared to systemic application. The next step will be to determine the clinical efficacy of local MSC-therapy in patients with active proctitis.

Acknowledgements
The authors thank Marij Mieremet-Ooms and Johan van der Reijden for excellent technical assistance. We thank Dr. Madelon Paauwe for providing the lentiviral luciferase construct and Dr. Jamie Lee for providing the MBP antibody.

REFERENCES

1. Loftus EV, Jr., Schoenfeld P, Sandborn WJ. The epidemiology and natural history of Crohn's disease in population-based patient cohorts from North America: a systematic review. Alimentary pharmacology & therapeutics. 2002;16:51-60
2. Burisch J, Jess T, Martinato M, et al. The burden of inflammatory bowel disease in Europe. Journal of Crohn's & colitis. 2013;7:322-337
3. Baumgart DC, Sandborn WJ. Crohn's disease. The Lancet. 2012;380:1590-1605
4. Ordás I, Eckmann L, Talamini M, et al. Ulcerative colitis. The Lancet. 2012;380:1606-1619
5. Frolkis AD, Dykeman J, Negron ME, et al. Risk of surgery for inflammatory bowel diseases has decreased over time: a systematic review and meta-analysis of population-based studies. Gastroenterology. 2013;145:996-1006
6. Gibson PR, Weston AR, Shann A, et al. Relationship between disease severity, quality of life and health-care resource use in a cross-section of Australian patients with Crohn's disease. Journal of gastroenterology and hepatology. 2007;22:1306-1312
7. Casellas F, Lopez-Vivancos J, Casado A, et al. Factors affecting health related quality of life of patients with inflammatory bowel disease. Quality of life research : an international journal of quality of life aspects of treatment, care and rehabilitation. 2002;11:775-781
8. Molendijk I, Bonsing BA, Roelofs H, et al. Allogeneic Bone Marrow-Derived Mesenchymal Stromal Cells Promote Healing of Refractory Perianal Fistulas in Patients With Crohn's Disease. Gastroenterology. 2015;149:918-927 e916
9. Panes J, Garcia-Olmo D, Van Assche G, et al. Expanded allogeneic adipose-derived mesenchymal stem cells (Cx601) for complex perianal fistulas in Crohn's disease: a phase 3 randomised, double-blind controlled trial. Lancet (London, England). 2016;388:1281-1290
10. Chinnadurai R, Copland IB, Ng S, et al. Mesenchymal Stromal Cells Derived From Crohn's Patients Deploy Indoleamine 2,3-dioxygenase-mediated Immune Suppression, Independent of Autophagy. Mol Ther. 2015;23:1248-1261
11. Prevosto C, Zancolli M, Canevali P, et al. Generation of CD4+ or CD8+ regulatory T cells upon mesenchymal stem cell-lymphocyte interaction. Haematologica. 2007;92:881-888
12. Luz-Crawford P, Kurte M, Bravo-Alegria J, et al. Mesenchymal stem cells generate a CD4+CD25+Foxp3+ regulatory T cell population during the differentiation process of Th1 and Th17 cells. Stem Cell Res Ther. 2013;4:65
13. Nauta AJ, Fibbe WE. Immunomodulatory properties of mesenchymal stromal cells. Blood. 2007;110:3499-3506
14. Carty F, Mahon BP, English K. The influence of macrophages on mesenchymal stromal cell therapy: passive or aggressive agents? Clinical and experimental immunology. 2017;188:1-11
15. Gonzalez-Rey E, Anderson P, Gonzalez MA, et al. Human adult stem cells derived from adipose tissue protect against experimental colitis and sepsis. Gut. 2009;58:929-939
16. Semont A, Mouiseddine M, Francois A, et al. Mesenchymal stem cells improve small intestinal integrity through regulation of endogenous epithelial cell homeostasis. Cell death and differentiation. 2010;17:952-961
17. Molendijk I, Barnhoorn MC, de Jonge-Muller ES, et al. Intraluminal Injection of Mesenchymal Stromal Cells in Spheroids Attenuates Experimental Colitis. Journal of Crohn's & colitis. 2016;10:953-964
18. Cooper HS, Murthy SN, Shah RS, et al. Clinicopathologic study of dextran sulfate sodium experimental murine colitis. Laboratory investigation; a journal of technical methods and pathology. 1993;69:238-249
19. Hawinkels LJ, Paauwe M, Verspaget HW, et al. Interaction with colon cancer cells hyperactivates TGF-beta signaling in cancer-associated fibroblasts. Oncogene. 2014;33:97-107
20. Hawinkels LJ, Verspaget HW, van Duijn W, et al. Tissue level, activation and cellular localisation of TGF-beta1 and association with survival in gastric cancer patients. British journal of cancer. 2007;97:398-404

21. Holmannova D, Kolackova M, Kondelkova K, et al. CD200/CD200R paired potent inhibitory molecules regulating immune and inflammatory responses; Part I: CD200/CD200R structure, activation, and function. Acta medica (Hradec Kralove). 2012;55:12-17
22. Liu X, Duan B, Cheng Z, et al. SDF-1/CXCR4 axis modulates bone marrow mesenchymal stem cell apoptosis, migration and cytokine secretion. Protein & cell. 2011;2:845-854
23. Muzaki AR, Tetlak P, Sheng J, et al. Intestinal CD103(+)CD11b(-) dendritic cells restrain colitis via IFN-gamma-induced anti-inflammatory response in epithelial cells. Mucosal immunology. 2016;9:336-351
24. Bartosh TJ, Ylostalo JH, Mohammadipoor A, et al. Aggregation of human mesenchymal stromal cells (MSCs) into 3D spheroids enhances their antiinflammatory properties. Proceedings of the National Academy of Sciences of the United States of America. 2010;107:13724-13729
25. Waterman RS, Tomchuck SL, Henkle SL, et al. A new mesenchymal stem cell (MSC) paradigm: polarization into a pro-inflammatory MSC1 or an Immunosuppressive MSC2 phenotype. PloS one. 2010;5:e10088
26. Sala E, Genua M, Petti L, et al. Mesenchymal Stem Cells Reduce Colitis in Mice via Release of TSG6, Independently of Their Localization to the Intestine. Gastroenterology. 2015;149:163-176 e120
27. Manieri NA, Mack MR, Himmelrich MD, et al. Mucosally transplanted mesenchymal stem cells stimulate intestinal healing by promoting angiogenesis. J Clin Invest. 2015;125:3606-3618
28. Farin HF, Karthaus WR, Kujala P, et al. Paneth cell extrusion and release of antimicrobial products is directly controlled by immune cell-derived IFN-gamma. The Journal of experimental medicine. 2014;211:1393-1405
29. Tanaka K, Ichiyama K, Hashimoto M, et al. Loss of suppressor of cytokine signaling 1 in helper T cells leads to defective Th17 differentiation by enhancing antagonistic effects of IFN-gamma on STAT3 and Smads. Journal of immunology (Baltimore, Md : 1950). 2008;180:3746-3756
30. Lim JY, Im KI, Lee ES, et al. Enhanced immunoregulation of mesenchymal stem cells by IL-10-producing type 1 regulatory T cells in collagen-induced arthritis. Scientific reports. 2016;6:26851
31. Ciccocioppo R, Cangemi GC, Kruzliak P, et al. Ex vivo immunosuppressive effects of mesenchymal stem cells on Crohn's disease mucosal T cells are largely dependent on indoleamine 2,3-dioxygenase activity and cell-cell contact. Stem Cell Res Ther. 2015;6:137
32. Schepers K, Fibbe WE. Unraveling mechanisms of mesenchymal stromal cell-mediated immunomodulation through patient monitoring and product characterization. Annals of the New York Academy of Sciences. 2016;1370:15-23
33. Ren G, Su J, Zhang L, et al. Species variation in the mechanisms of mesenchymal stem cell-mediated immunosuppression. Stem cells (Dayton, Ohio). 2009;27:1954-1962

SUPPLEMENTARY FILES

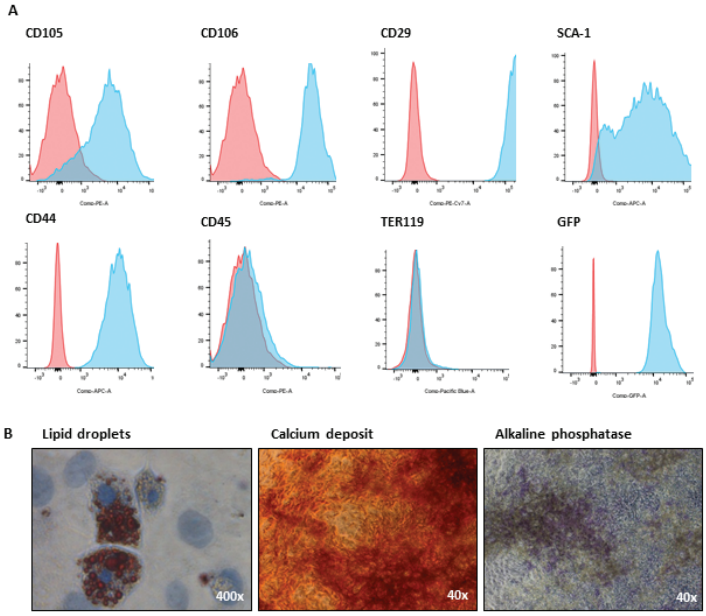

Supplementary FIGURE 1. Phenotypical characterization of MSCs. (A): Flow cytometry shows that surface markers CD105, CD106, CD29, SCA-1, CD44 and GFP are present on MSCs, while CD45 and TER119 are absent. (B): MSCs are able to differentiate into adipocytes (lipid droplets) and osteoblasts (calcium deposit and alkaline phosphatase activity).

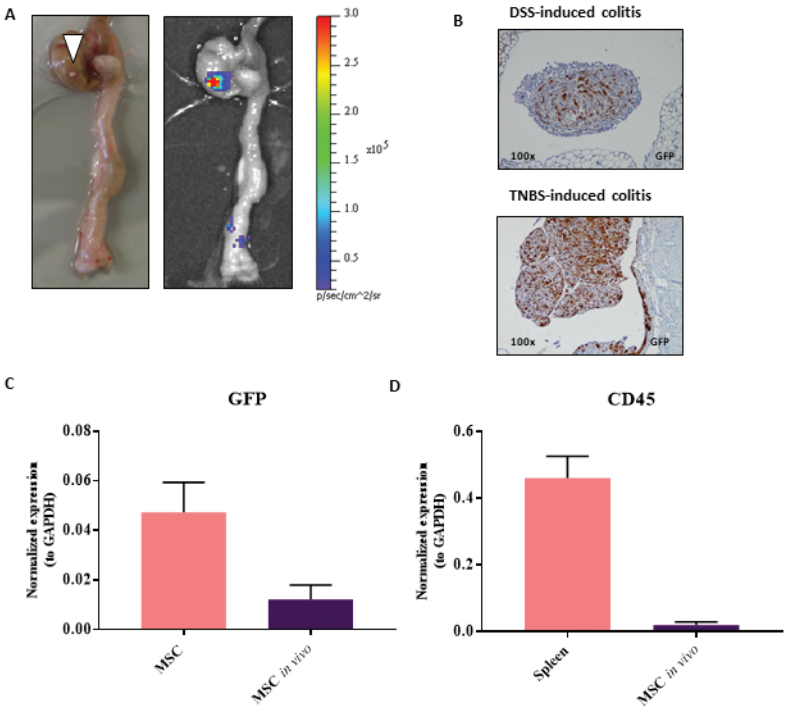

Supplementary FIGURE 2. Abdominal MSC-aggregates contain mainly MSCs and a low level of immune cells. (A): Bioluminescent imaging confirms the presence of a MSC-aggregate on the cecum (white arrowhead), 5 days after intraperitoneal injection. (B): Immunohistochemically staining for GFP shows MSC-aggregates in the abdomen of mice with DSS-induced and TNBS-induced colitis. Magnification x100. (C/D): qPCR shows a substantial level of GFP (C) and a low level of CD45 (B) expression in *in vivo* MSC-aggregates compared with respectively *in vitro* MSCs or spleens. Expression levels are measured in triplicate and normalized to GAPDH. Data are expressed as mean ± SEM

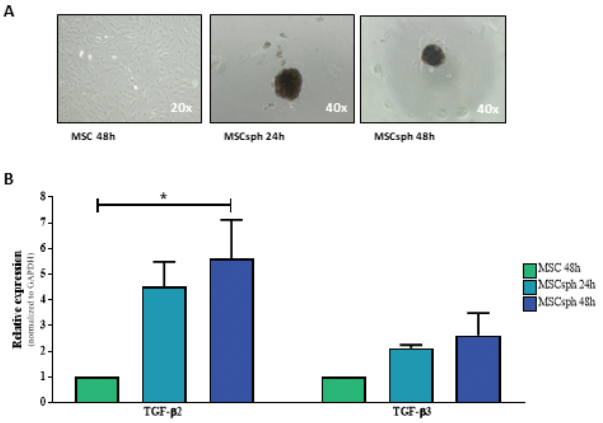

.

Supplementary FIGURE 3. TGF-β2 is significantly upregulated in MSC-spheroids (A): *In vitro* MSCs cultured for 48 hours (MSC 48h) in monolayer and in spheroids for 24 (MSCsph 24h) and 48 hours (MSCsph 48h). Magnification 20x (MSC 48h) and 40x (MSCsph 24h and 48H). (B): qPCR comparing expression levels of MSC 48h, MSCsph 24h and MSCsph 48h for TGF-β2 and TGF-β3. The data are the result of 6 independent experiments in triplicate. Expression levels are normalized to GAPDH and compared to MSC 48h. Data are expressed as mean ± SEM. *p ≤ 0.05.

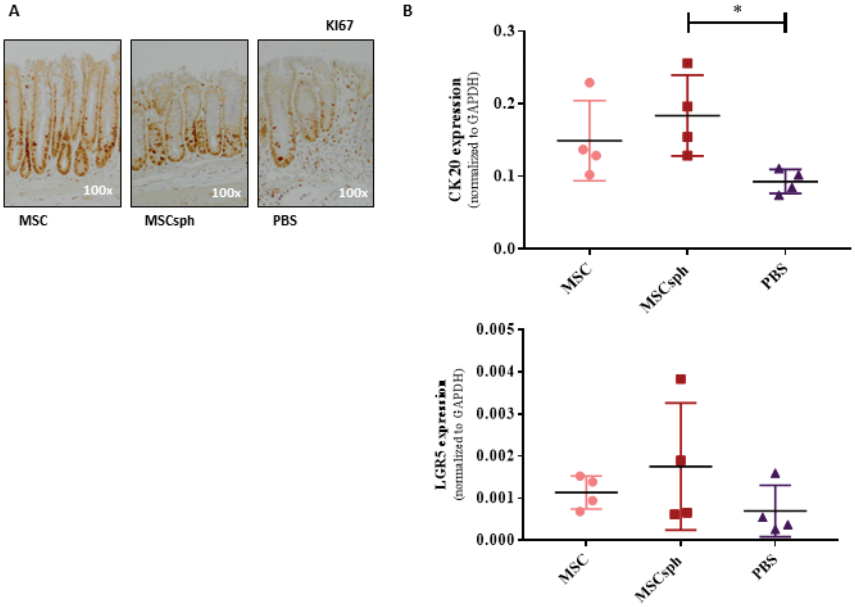

Supplementary FIGURE 4. The stem cell compartment in the colon is not affected by MSC-therapy (A): Immunohistochemically staining for Ki67 shows normal crypt proliferation in MSC- and PBS-treated mice. (B): qPCR comparing expression levels of CK20 and LGR5 in the colon of mice treated with MSCs, MSC-spheroids or PBS.

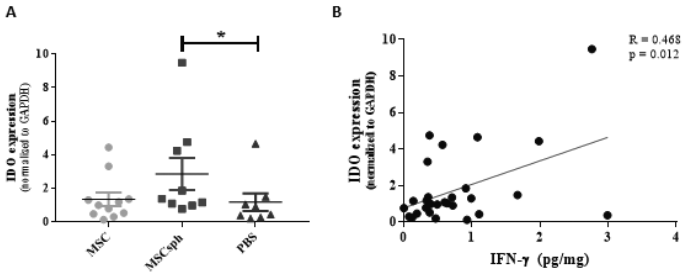

Supplementary FIGURE 5. IDO is upregulated in colons of mice 4 days after treatment with MSC-spheroids. (A): RNA expression levels of IDO are elevated in mice that received MSC-spheroids 4 days after therapy. Data are expressed as mean ± SEM. *$p \leq 0.05$. (B): IFN-γ levels in the colon, 4 days after treatment, are significantly correlated with IDO expression levels, $R = 0.468$, $p \leq 0.05$.

LIST OF SUPPLEMENTARY DIGITAL CONTENT

Supplementary Digital Content 1 – Table of primer sequences.

Supplementary Digital Content 2 – Video that demonstrates endoscopic bowel wall injection of MSCs.